Electronic Structure of the Perovskite Oxides: $La_{1-x}Ca_xMnO_3$

S. Satpathy
Department of Physics and Astronomy, University of Missouri, Columbia, Missouri 65211

Zoran S. Popović and Filip R. Vukajlović
Laboratory for Theoretical Physics, Institute of Nuclear Sciences-"Vinča," 11001 Belgrade, Yugoslavia
(Received 18 May 1995)

The electronic structures of the perovskite oxides, $LaMnO_3$ and $CaMnO_3$, are studied using density-functional methods. Antiferromagnetic insulating (AFI) solutions are obtained for both compounds within the local-density approximation (LDA). For $LaMnO_3$ the Jahn-Teller distortion, found necessary for the AFI solution, produces occupied Mn($z^2 - 1$) orbitals pointed along the long, basal-plane Mn-O bonds. The large on-site Coulomb U and exchange J, obtained from "constrained" LDA calculations, $U \approx 8-10$ eV and $J \approx 0.9$ eV, indicate important correlation effects and yield large redistribution of the spectral weight within the LDA + U approach.

PACS numbers: 71.20.Ps, 71.70.–d, 75.50.Ee

The rich variety of electrical conduction exhibited by the transition-metal oxides has made them a lively area of research over the last several decades [1,2]. These include compounds such as NiO, the classic Mott insulator, Fe_3O_4 which shows the Verwey charge-ordering transition, ReO_3 with room-temperature conductivity as large as that of copper, and the more recent high-T_c copper-oxide superconductors. This Letter deals with the perovskite oxides, viz., the lanthanum manganite and its calcium doped alloys, $La_{1-x}Ca_xMnO_3$, a topic of considerable renewed interest following the discovery of colossal magnetoresistance (CMR) in the La-Ca-Mn-O and related films [3,4]. Apart from the CMR effects, the unusual magnetic and conduction properties of the lanthanum manganites are well known. For example, $La_{1-x}Ca_xMnO_3$ is a ferromagnetic conductor in the range of $0.2 < x < 0.4$, while the end members, $x = 0$ or 1, are antiferromagnetic (AF) insulators [5]. The simultaneous occurrence of ferromagnetism and metallic conduction is qualitatively explained with Zener's idea of double exchange, where the presence of the Mn^{3+}-Mn^{4+} mixed valence ions is responsible for both ferromagnetic coupling and charge transport [6].

Both $LaMnO_3$ and $CaMnO_3$ are AF insulators, but while in $LaMnO_3$ stacks of ferromagnetic (001) planes are arranged antiferromagnetically (type A, according to the Wollan-Koehler classification [7]), in $CaMnO_3$, each Mn atom is surrounded by six nearest neighbors with AF alignment (type G). Here, we examine the electronic structure of these perovskites from density-functional calculations within the local spin-density approximation (LDA) as well as the "constrained" density-functional and the LDA + U approaches [8], using the linear muffin-tin orbitals (LMTO-ASA) method [9].

An important structural feature of the perovskite oxides is the presence of the oxygen octahedra, which may be distorted. Both $LaMnO_3$ and $CaMnO_3$ form in the orthorhombic crystal structure [10], which is a distorted form of the cubic perovskite structure (Fig. 1). The O octahedron in $LaMnO_3$ contains a strong static Jahn-Teller (JT) distortion, while in $CaMnO_3$ this distortion is small. The JT distortion consists of a combination of the three modes that change the Mn-O bond lengths, viz., the breathing mode Q_1, the basal-plane distortion mode Q_2, and the octahedral stretching mode Q_3 [11], plus a small rotation of the O octahedron, resulting in the Mn-O bond lengths of 1.91, 2.19, and 1.96 Å for $LaMnO_3$. We performed the LDA calculations for the observed crystal structure for $LaMnO_3$ as well as for the ideal perovskite structures with only specific JT modes included. Only the ideal cubic structure was studied for $CaMnO_3$, where the JT distortion is small. The AF unit cell has four formula units for $LaMnO_3$, while it has two formula units for $CaMnO_3$.

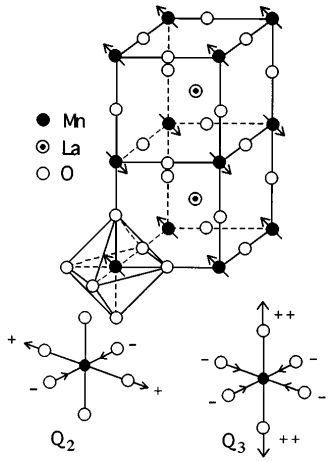

FIG. 1. The ideal cubic perovskite structure, showing the AF type A order for $LaMnO_3$. In the actual structure, the oxygen octahedron is distorted with a combination of the breathing mode (Q_1), the basal-plane distortion mode (Q_2), and the octahedral stretching mode (Q_3) in addition to a small rotation of the octahedron.

 0031-9007/96/76(6)/960(4)$06.00

The energy bands of $LaMnO_3$ in the observed crystal structure and AF type *A* order are shown in Fig. 2(a). The Mn($3d$) bands occur above O($2p$) bands much like in MnO [12]. In agreement with the conventional wisdom, we find the nominal chemical formula, $La^{3+}Mn^{3+}O_3{}^{2-}$, with the La and Mn outer electrons transferred to the oxygen atom to complete the $2p$ shell. There is a small indirect gap between the JT-split Mn($3d$) e_g^1 and e_g^2 bands. The band positions as well as the moderate hybridization between the O and the Mn bands are seen from the partial densities of states (DOS) shown in Fig. 3.

We find that the occupied, majority spin $e_g^1\uparrow$ bands are derived from the Mn(z^2-1) orbitals, in a Mn-atom-based *local* coordinate system, with the z axis pointed along the long Mn-O bond on the basal plane. Figure 2(a) inset shows the contribution of these orbitals to the electron bands. The occupation of the Mn(z^2-1) orbitals is also noticeable from the charge-density contours shown in Fig. 4. The same conclusion concerning orbital occupancy was derived from a recent Hartree-Fock model study [13].

As seen from Fig. 2(a), the $e_g^1\uparrow$ bands are about 1.0 eV wide, while the $t_{2g}\uparrow$ bands, just below $e_g^1\uparrow$, are about 1.2 eV wide. However, as indicated from the excursion of the Mn(z^2-1) orbital components into the $t_{2g}\uparrow$ bands, the doped holes in the mixed compound $La_{1-x}Ca_xMnO_3$ are to be considered as having a much larger width, of about 2.0 eV, than the width of just the $e_g^1\uparrow$ bands would suggest.

Without the JT distortion, $LaMnO_3$ in the ideal cubic structure has metallic bands with the Fermi energy E_f lying in the middle of the e_g bands. However, in view of the $t_{2g}^3e_g^1$ configuration of the Mn atom, a symmetry-breaking JT distortion is expected [14], and this is observed experimentally. We find that for $LaMnO_3$ a JT distortion of the Q_2 type, with the basal-plane oxygen atoms displaced by at least the amount $\approx$0.1 Å from their ideal positions (experimental value of this distortion is $\approx$0.15 Å), is necessary for

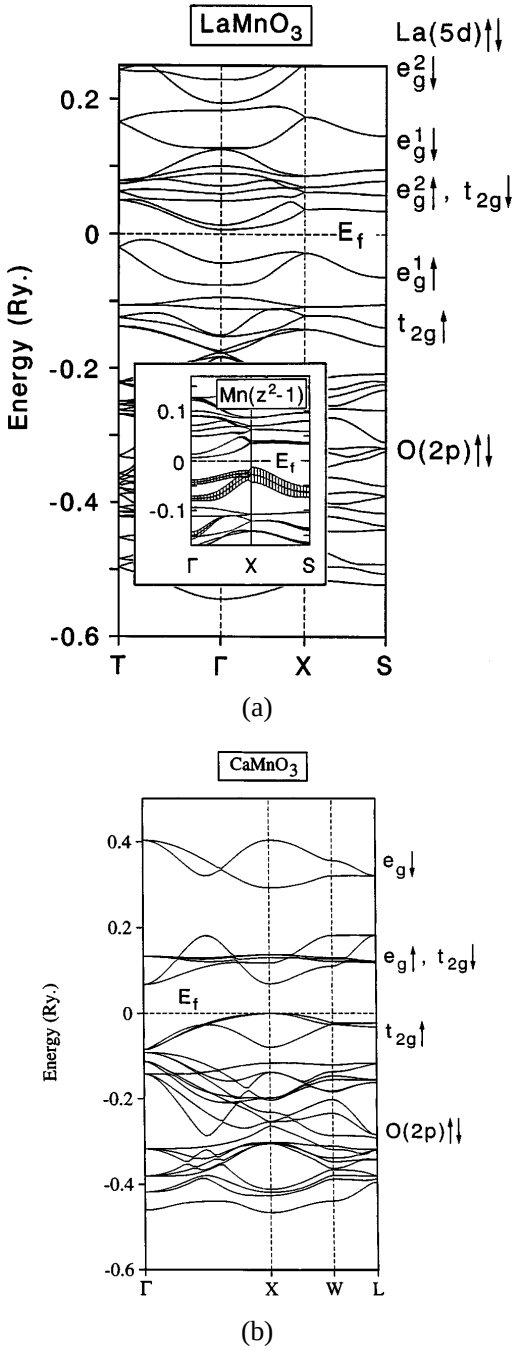

FIG. 2. Band structures of $LaMnO_3$ (AF type *A*) in the observed crystal structure (a) and of $CaMnO_3$ (AF type *G*) in the tetragonal crystal structure (b). The e_g and t_{2g} components correspond to the Mn($3d$) orbital. In the inset of (a), each band state is given a width, by vertical hatching, proportional to the contribution of the majority spin Mn(z^2-1) orbitals in a local coordinate system with the z axis pointed along the long, basal-plane Mn-O bonds. A 35 mRy width equals 100% contribution. Significant contribution is seen only for the $e_g^1\uparrow$ bands and for one band around the Γ point in the $t_{2g}\uparrow$ group of bands.

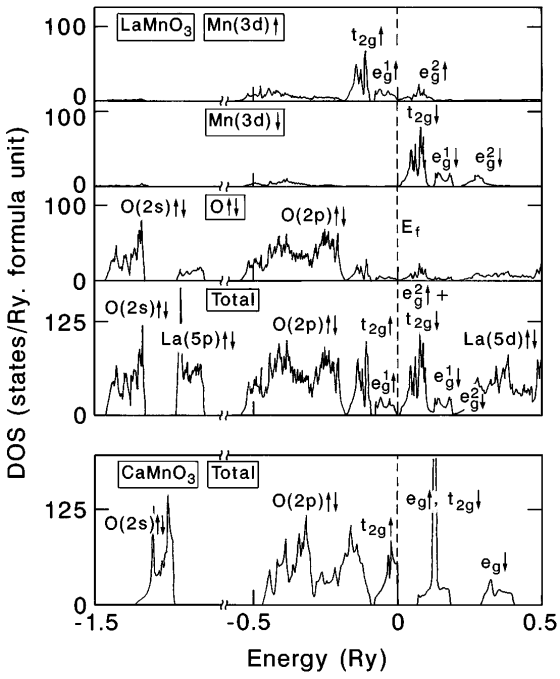

FIG. 3. The total and partial densities of states for $LaMnO_3$ and $CaMnO_3$ obtained from LDA calculations.

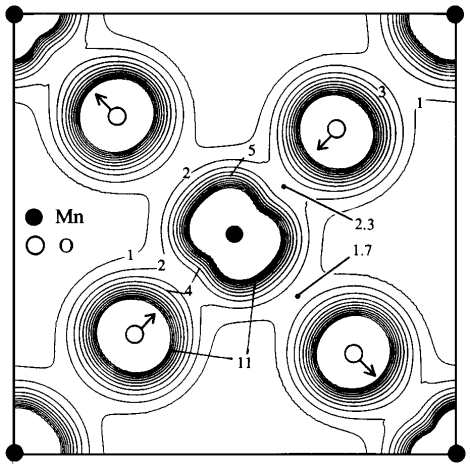

FIG. 4. Electronic valence charge-density contour plot on the basal plane of $LaMnO_3$. Arrows on the oxygen atoms indicate the Q_2-type JT distortion. Contour values are in units of $1.8 \times 10^{-2}\ e^-/(\text{Bohr radius})^3$.

an insulating band structure within the LDA and that the Q_1 or the Q_3 distortions are not effective in opening up the gap. The JT distortion furthermore stabilizes the AF structure over the ferromagnetic structure [15].

The band structure for the other end member, $CaMnO_3$, is shown in Fig. 2(b). We obtain an AF insulating solution here as well with the nominal chemical formula, $Ca^{2+}Mn^{4+}O_3{}^{2-}$, and the experimentally observed G type AF order. The Mn valency is now Mn^{4+} with the $t_{2g}^3 e_g^0$ configuration. No JT distortion is expected, and none is necessary to produce an insulating gap.

The basic picture that emerges then for the mixed compound $La_{1-x}Ca_xMnO_3$ is that the $Mn(z^2 - 1)$ band, which is completely filled for $x = 0$, is progressively depleted with the increase of the Ca concentration x, with complete depletion for $x = 1$. The band picture is therefore consistent with the fact that both end members are insulators while the intermediate compounds are conductors. For the intermediate compounds, the mobile electrons in the e_g^1 bands couple the t_{2g} spins ferromagnetically via double exchange, even though in contrast to the standard double-exchange model, the t_{2g} electrons in the band picture do have a substantial bandwidth.

Electron correlation effects are well known to be important for the transition-metal binary oxides. To assess the importance of correlation for the perovskites, we have estimated the on-site Coulomb (U) and the intra-atomic exchange (J) parameters for the Mn atom from "constrained" density-functional calculations [16–18]. In these calculations, the occupancy of the d electrons on the central Mn atom was constrained in a 4-formula-unit supercell, with the hopping integral between these electrons and the rest of the system set equal to zero. All electrons except the constrained d electrons thus contribute to screening. Fresh self-consistent LDA calculations were performed with the constraint and the electron interaction parameters were obtained from the Slater's transition rules [10],

$$U = \varepsilon_{3d\uparrow}\left(\frac{n^0}{2} + \frac{1}{2}, \frac{n^0}{2}\right) - \varepsilon_{3d\uparrow}\left(\frac{n^0}{2} + \frac{1}{2}, \frac{n^0}{2} - 1\right) \tag{1}$$

and

$$J = \varepsilon_{3d\downarrow}\left(\frac{n^0}{2} + \frac{1}{2}, \frac{n^0}{2} - \frac{1}{2}\right) - \varepsilon_{3d\uparrow}\left(\frac{n^0}{2} + \frac{1}{2}, \frac{n^0}{2} - \frac{1}{2}\right), \tag{2}$$

where $\varepsilon_{3d\sigma}(n_{d\uparrow}, n_{d\downarrow})$ are self-consistent eigenenergies of the $3d$ orbitals of the central Mn atom, calculated for the fixed spin occupancies, $n_{d\uparrow}$ and $n_{d\downarrow}$, and n^0 is the number of $3d$ electrons on the central Mn site without any constraint.

The calculated U and J values are given in Table I. Not surprisingly, both $LaMnO_3$ and $CaMnO_3$ have similar values: $U \approx 10$ eV and $J \approx 0.9$ eV. This is in view of the fact that both La and Ca merely donate their outer electrons to the system, with their orbitals far removed from E_f, so that these atoms do not contribute much to the screening. Now, in the LMTO-ASA calculation, the Coulomb interaction may be somewhat underscreened because the screening charges reside at the sphere centers. An upper bound for this error may be obtained by placing the screening charges of the neighboring atoms at the surface of the central Mn sphere [19], which yields a value of about 2.1 eV in the present case. Thus our results indicate a U value of about 8–10 eV, which is consistent with the estimate of $U \simeq 7.5$ eV from photoemission [20].

We note that the bare U_{at} for the Mn atom, of about 20 eV as obtained from the electrostatic atomic integral, is reduced to only about $U_{\text{at}}^{\text{rel}} \approx 12.8$ eV, with relaxation effects of the atomic shells included. Screening by the conduction electrons further reduces the value of U in the solid; some values reported in the literature are $U \approx 6.9$ eV (MnO) [8] and $U \approx 7.8$ eV (Mn in ZnTe) [18], which are similar to our calculated value for the manganese perovskites. The calculated exchange parameter $J \approx 0.88$ eV is typical of the transition-metal oxides, where it varies between 0.78 and 0.98 eV [8].

With the calculated Coulomb and exchange parameters, we have minimized the LDA + U functional, which takes into account the effects of the large Hubbard U term in a mean-field sense. Although this is not a substitute for a true many-body solution, the LDA + U results do provide important guidelines. In Fig. 5, we summarize the results of the LDA + U calculations by showing a

TABLE I. Calculated intrasite Coulomb and exchange parameters (in eV) and magnetic moments (in units of μ_B).

	U	J	μ_{LDA}	$\mu_{\text{LDA}+U}$	μ_{exp}
$LaMnO_3$	10.1	0.88	3.48	4.0	3.7 ± 0.1 [10]
$CaMnO_3$	10.0	0.86	2.62	3.3	2.7 [7]

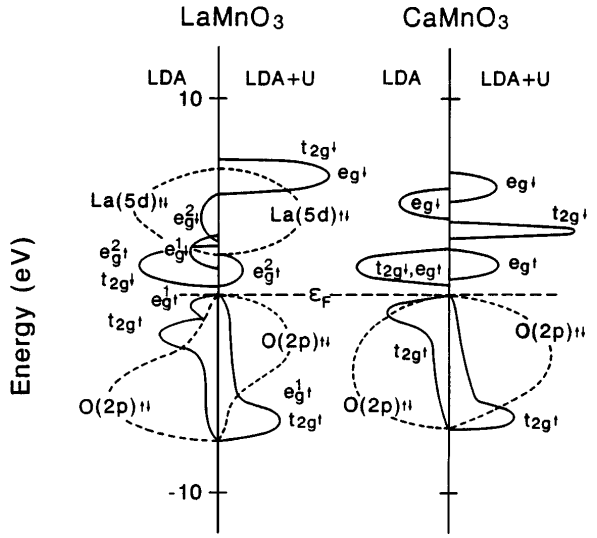

FIG. 5. Sketch of the one-electron densities of states extracted from the LDA and the LDA + U calculations.

sketch of the one-electron DOS. The spectral weight is considerably redistributed. In particular, while the Mn($3d$) band center occurs above the O($2p$) in the LDA, in the LDA + U results this is reversed. The occupied Mn($3d$) states are separated from the unoccupied ones by an energy of order U.

The valence-band photoemission spectra for $LaMnO_3$ show a broad O($2p$)-Mn($3d$) double-peak structure of about 7 eV width [21,22], consistent with *both* the LDA and the LDA + U results. The photoemission spectra have been modeled by two groups [20,21] who obtain somewhat different values for the electron parameters. Our LDA + U results, which put the O($2p$) level above Mn($3d$), are in better agreement with the parameter values of Bocquet *et al.* [20], which with an $U \simeq 7.5$ eV would put these oxides in the charge-transfer insulator regime [23]. The large value of U as compared to the bandwidth does indicate strong many-body effects, which is reflected, for example, in the Mn($2p$) core-level photoemission spectra, where a satellite peak is seen at the binding energy of $\approx$10 eV [20,21]. The enhancement of the magnetic moment (Table I), although overestimated in the LDA + U result, is indicative of an oxygen ligand hole admixture in the ground state, e.g., of the type $|d^4\rangle + a|d^5\underline{L}\rangle$ for $LaMnO_3$.

In conclusion, even though within the local-density theory antiferromagnetic insulating solutions are obtained for both $LaMnO_3$ and $CaMnO_3$, we have argued that these are strongly correlated systems. The important JT distortion for $LaMnO_3$ is of the Q_2 type, which is essential for the insulating gap within the LDA. For the mixed compound, $La_{1-x}Ca_xMnO_3$, the JT-split Mn($3d$) e_g^1 band is gradually depleted with increasing x, with a complete depletion occurring for $CaMnO_3$. The Coulomb interaction U is strong enough that we expect significant correlation, which is reflected in the considerable redistribution of the spectral weight in the LDA + U results and also it is reflected in the results of the photoemission experiments.

We thank O. Gunnarsson for stimulating discussions. This work was supported in part by the Office of Naval Research under Contract No. ONR N00014-95-1-0439.

[1] N. F. Mott, *Metal-Insulator Transitions* (Taylor and Francis, London, 1974).
[2] B. Brandow, Adv. Phys. **26**, 651 (1977).
[3] R. von Helmolt, J. Wecker, B. Holzapfel, L. Schultz, and K. Samwer, Phys. Rev. Lett. **71**, 2331 (1993).
[4] S. Jin, T. H. Tiefel, M. McCormack, R. A. Fastnacht, R. Ramesh, and L. H. Chen, Science **264**, 413 (1994).
[5] G. H. Jonker and J. H. Van Santen, Physica (Utrecht) **16**, 337 (1950); J. H. Van Santen and G. H. Jonker, Physica (Utrecht) **16**, 599 (1950).
[6] C. Zener, Phys. Rev. **82**, 403 (1951); P. W. Anderson and H. Hasegawa, Phys. Rev. **100**, 675 (1955); P.-G. de Gennes, Phys. Rev. **118**, 141 (1960).
[7] E. O. Wollan and W. C. Koehler, Phys. Rev. **100**, 545 (1955).
[8] V. Anisimov, J. Zaanen, and O. K. Andersen, Phys. Rev. B **44**, 943 (1991).
[9] O. K. Andersen, Phys. Rev. B **12**, 3060 (1975).
[10] J. B. A. A. Elemans, B. van Laar, K. R. van der Veen, and B. O. Loopstra, J. Solid State Chem. **3**, 238 (1971).
[11] M. D. Sturge, in *Solid State Physics*, edited by F. Seitz, D. Turnbull, and H. Ehrenreich (Academic Press, New York, 1967), Vol. 20.
[12] M. Arai and T. Fujiwara, Phys. Rev. B **51**, 1477 (1995); K. Terakura, T. Oguchi, A. R. Williams, and J. Kübler, Phys. Rev. B **30**, 4734 (1984); O. K. Andersen and S. Satpathy, in *Properties of Binary Oxides*, edited by A. D. Rodriguez, J. Castaing, and R. Marquez (Universidad de Sevilla, Spain, l984).
[13] T. Mizokawa and A. Fujimori, Phys. Rev. B **51**, 12 880 (1995).
[14] J. B. Goodenough, Phys. Rev. **100**, 564 (1955).
[15] W. E. Pickett and D. J. Singh, Phys. Rev. B (to be published).
[16] P. H. Dederichs, S. Blügel, R. Zeller, and H. Akai, Phys. Rev. Lett. **53**, 2512 (1984).
[17] A. K. McMahan, R. M. Martin, and S. Satpathy, Phys. Rev. B **38**, 6650 (1988).
[18] O. Gunnarsson, O. K. Andersen, O. Jepsen, and J. Zaanen, Phys. Rev. B **39**, 1708 (1989).
[19] V. Drchal, O. Gunnarsson, and O. Jepsen, Phys. Rev. B **44**, 3518 (1991).
[20] A. E. Bocquet, T. Mizokawa, T. Saitoh, H. Namatame, and A. Fujimori, Phys. Rev. B **46**, 3771 (1992).
[21] A. Chainani, M. Matthew, and D. D. Sarma, Phys. Rev. B **47**, 15 397 (1993).
[22] D. D. Sarma, N. Shanthi, S. R. Barman, N. Hamada, H. Sawada, and K. Terakura, Phys. Rev. Lett. **75**, 1126 (1995).
[23] J. Zaanen, G. A. Sawatzky, and J. W. Allen, Phys. Rev. Lett. **55**, 418 (1985).